Radiation Imaging Techniques

Ionizing Radiation

- Radiations from atomic/nuclear processes
- In nuclear science and technology: 10 eV – 20 MeV
- Charged particles
  - Fast electrons ($\beta^{\pm}$)
  - Heavy charged particles (p, d, t, α, fission products)
- Neutral particles
  - Electromagnetic waves
    - · X-rays: transition between e^- shells of atoms
    - · γ-rays: nuclear energy level transition
  - Neutrons: thermal, slow, epithermal, fast neutrons
- Other charged particles and neutral particles may exist.

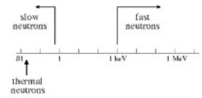

Radiation Detection & Measurement

Ionizing Radiation

- **We "detect" (existence)**
  - **Charged particles (α, β), neutral particles (γ, n, ν)**
  - **Non-ionizing radiation**
- **We "measure" (known existence)**
  - **Energy spectrum: energy given to the detection media**
- **And could we "sense" ?**
  - **Position and timing: requires signal processing**
- **Then we can "visualize" invisible things (imaging)**
  - **Incident direction via imaging methods**
  - **Radiography: X-ray, gamma ray, neutron, muon, etc.**

Radiation Detection & Measurement

- Interaction of radiation with matter
  - Interaction of charged particle with matter
    ; Stopping power, Range, Bragg curve, Bethe formula
  - Interaction of energetic photons with matter
    ; Photoelectric effect, Compton scattering, Pair production
  - Neutron interactions
    ; Scattering (Elastic, Inelastic), Absorption (Nuclear reaction)
- Radiation measurement
  - Event in detector → Energy deposition → Charge carriers
  - Measured current or voltage signal ∝ Radiation energy
  - Modes of detector operation ; pulse mode, current mode

(Ionizing) Radiation Detectors

- Higher demand for nuclear radiation detection; Homeland security, medical application, scientific researches etc.
- Radiation of interest; Ionizing radiation (α, β, γ, n)
- Principle; Signal induced from the motion of charge carriers created by (direct/indirect) ionizing mechanism of radiation.
- Typical energy range; Energy released from nuclear decay
  - a few MeVs for α, sub MeV to ~ 3 MeV for β and γ
- Energy Ranges by Applications
  - Homeland security; ~ MeV γ's and neutrons (slow/fast)
  - Medical application; 511 keV γ's for PET, x-rays, slow n's
  - Scientific research; wide range (CX meas., NAA, NRF, etc.)

Major Trends in RDM R&D (Hardware)

- Detection Materials
  - Scintillators: SrI_2, $CeBr_2$ (gammas), Elpasolites, Plastics (PSD)
  - Semiconductors: Compounds (TlBr, HgI_2) – RT Operation
  - Unconventional Detectors: Superconductors (TES)
- Detection Methods
  - Position Sensing combined with Imaging Methods
  - Neutron Detection (Fast and Slow) and Neutrino Detection
  - Electronics: Front-end (ASIC), Readouts (SSPM)
- Application
  - Medical Application: New RDM Methods in Application
  - Homeland Security: SNM Detection, Nuclear Safeguards
  - Scientific Research: Dark Matter Search, Particle Tracks

Radiographic Imaging

X-rays are used to examine the interior content of objects by recording and displaying transmitted radiation from a point-like source.

Detection Display

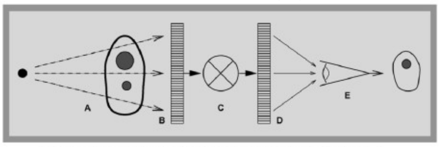

Subject contrast (A) recorded by the detector (B) is transformed (C) to display values and sent to a display device (D) for presentation to the human visual system (E) and interpretation.

It has been started from here:

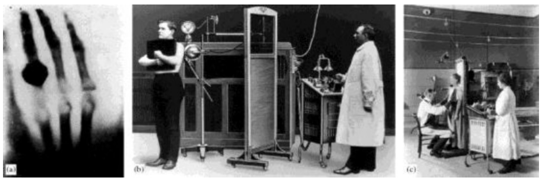

Fig. 1. (a) Ms. Röntgen's hand with ring (first X-ray image taken on December 22, 1895), (b) an early radiological workplace where the patient had to hold the film cassette himself, and (c) fluoroscopy in the Gynaecological Hospital, Erlangen (1918).

You can see through things!

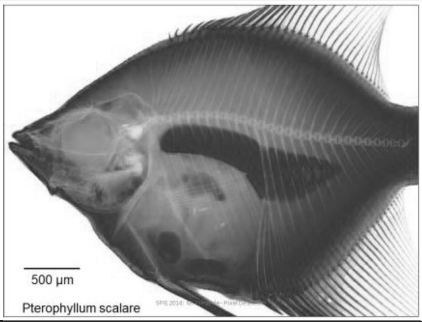

Like this..

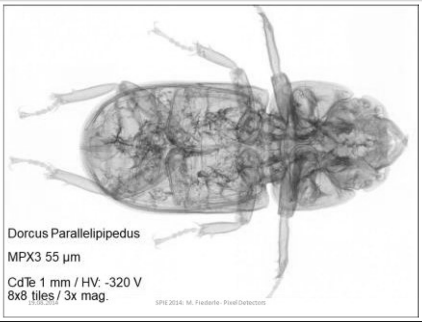

Even with High Resolution

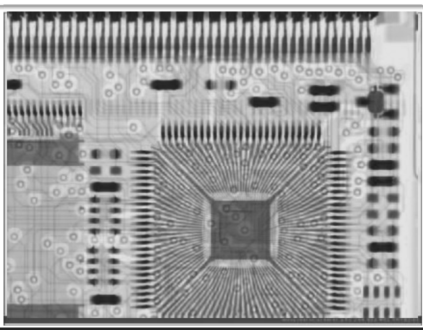

What could this be?

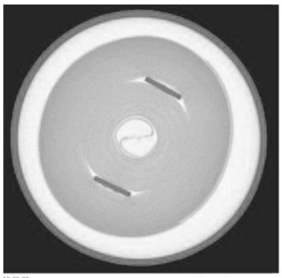

MPX3 55 µm
SPM HGM

GaAs 500 µm
HV: -280 V

2x4 tiles
No mag.

Then what about this?

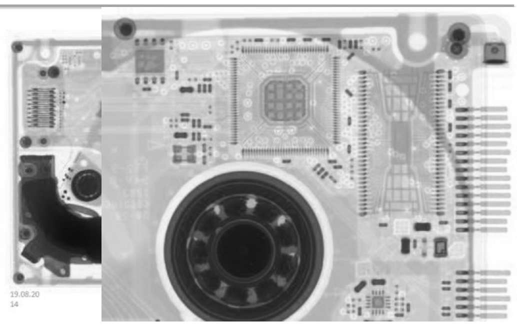

Some more techniques

Fig. 2. (a) Hand examination using a radiographic system (Siemens AXIOM Aristos FX®) comprising a flat-panel detector, (b) radiogram of a hand showing bones and nails, where soft tissue is barely visible, and (c) digital subtraction angiogram (DSA) of a hand with contrast media-filled vessels. The bones disappeared after subtraction of the native image, i.e. without contrast medium.

Dual-energy Technique

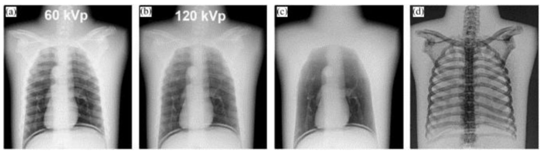

Fig. 4. Two chest radiograms taken with a **low** (a) and a **high** (b) **energy spectrum**. Applying an appropriate algorithm can make ribs and spine disappear and offer an undisturbed view on the **lung tissue** (c). Different weighting (d) leads to a bone image.

Energy Selective Imaging

RGB: 9-50 keV

Piezo Lighter

Magnification: 1.3x
Bias: -320V
MPX3 CdTe 1mm
Color Mode 4x11 tiles

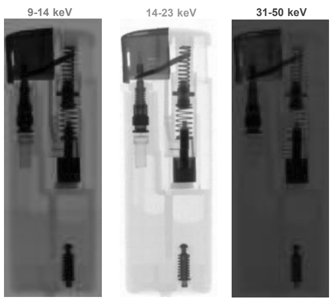

Transmission Geometry

The radiographic image formation process projects the properties of the object along straight lines from a point-like source to various positions on a detector surface.

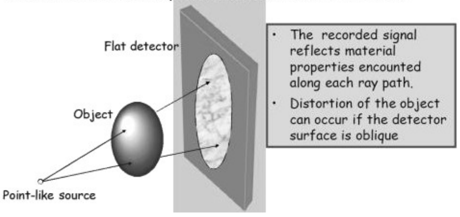

The radiographic project is a 'perspective transmissive projection' from the point of view of the source. Object features close to the source are magnified as are visual objects close to the viewer eye.

Enabling Technology

- Position-sensitive Detectors
- Detector Materials: Solid State Materials
- Readouts and electronics
- Measurement Techniques

Radioisotope Imaging

Radioisotope imaging differs from x-ray imaging only with respect to the source of radiation and the manner in which radiation reaches the detector

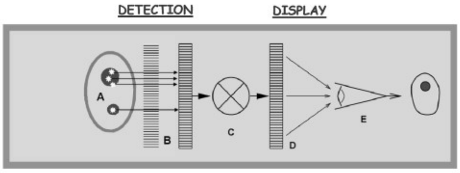

Pharmaceuticals tagged with radioisotopes accumulate in target regions. The detector records the radioactivity distribution by using a multi-hole collimator.

Contents from: M. Flynn, Principles of Radiation Imaging, University of Michigan

Radiation Imaging: Visualization of Radiation

- Nuclide information + Distribution of radioactivity

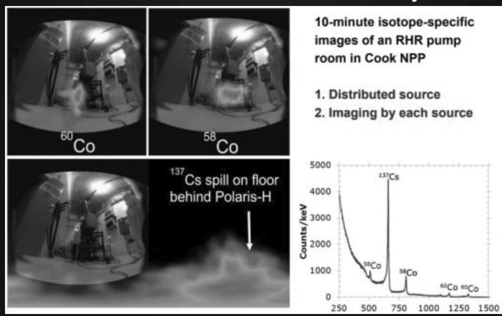

Images captured from H3Dgamma Inc.

Localization of radioactive hot spots

- Traditional method: "survey meter" or "radiation detector"
  - It provides only the presence of radioactivity
  - Possibility of overlooking locally existing hotspot
  - Long measurement time for quantification
  - Inevitable radiation exposure of the workers

- Radiation detection based on imaging technique
  - Visualization of spatial distribution of radioactivity (filling in blank area of traditional survey maps)
  - Monitoring the contaminated areas continuously

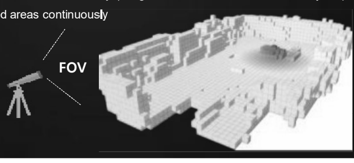

Imaging Concepts

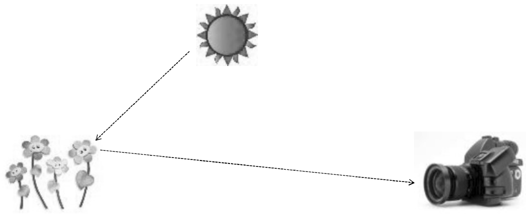

Optical Imaging

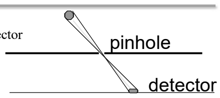

- The point-spread-function is a delta function
  - incident angle θ ↔ x on the position sensitive detector
- The limitation on angular resolution: $\Delta\theta = 1.22\dfrac{\lambda}{D}$
- If the wavelength $\lambda = 500$ nm $= 5\times10^{-7}$ m (visible light) and the diameter of the telescope D=10 m

$$\Delta\theta \approx \frac{5\times10^{-7}}{10} = 5\times10^{-8}$$

- For a 10 keV gamma-ray, $\lambda = \dfrac{hc}{E} = 1.24\times10^{-10}$ m
  - ~5000 times shorter ---- Great resolution?

So what is the limitation on angular resolution for gamma-rays?
- The challenge: the particle properties dominate!
- Gamma-ray imaging techniques: mostly rely on modulation of gamma-rays (except for Compton imagers and (focusing?)).

Pinhole Imaging

- Simple, but low efficiency
  - Requires 2-dimensional position sensitive detector
  - Angular resolution $\Delta\theta \approx \dfrac{D}{L}$
  - Pinhole means: D (hole diameter) > T (thickness of blocker)
    - (This limits its use to only low gamma-ray energies)
  - Want detector position resolution Δx ~ D
  - Detection efficiency
    - (Better angular resolution ↔ lower detection efficiency)

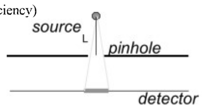

Mechanical Collimators

- **Parallel hole collimators (For close objects)**
  - (Such as SPECT gamma-cameras for bone-scan)
  - Higher resolution ↔ lower detection efficiency
  - No magnification on the objects (as a function of distance):
    - critical requirement for medical imaging
- **Diverging collimators (Low efficiency)**
  - For higher energy gamma-rays (thick collimators)
- **Converging collimators (Magnifying objects)**

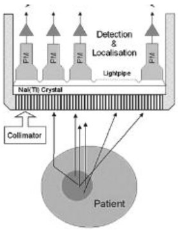

Mechanical Collimator Types

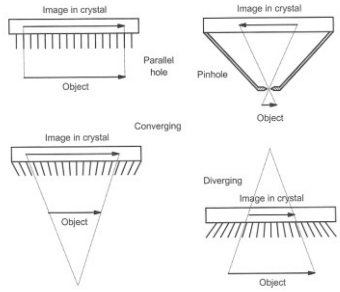

Modulation of Image – 1

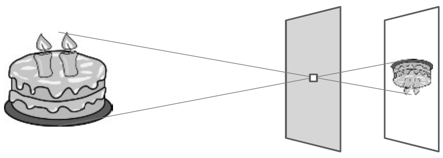

- A pinhole camera is very inefficient
- Most of the emitted radiation is blocked by the mask

Modulation of Image – 2

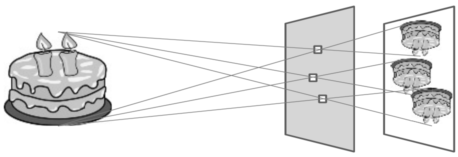

- Multiple pinholes increase the signal strength
- Images can be decoded by the mask pattern

Signal Modulation

- The idea is to open more than a single opening at a time
- improves efficiency
- Increases complexity of image reconstruction
- Masks:
  - Can modulate signal in space
    - e.g., coded masks
    - Detector may need to be position sensitive
  - or time
    - "Static" radiation field

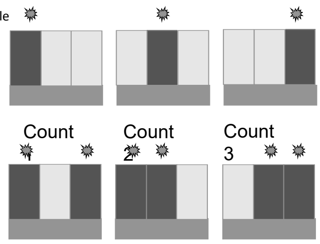

$$\begin{pmatrix} 1 & 0 & 1 \\ 1 & 1 & 0 \\ 0 & 1 & 1 \end{pmatrix}$$

Example: Signal Modulation

- Pair of collimators
- Slide one over other
  - Let dark=open=1
  - Form auto-correlation
    - {3,1,1,1,1,1,1}
    - Peak on constant background
- Move first and repeat
  - Result is a response matrix with only diagonal elements after bkgd subtraction
- Reconstruction using matrix operations

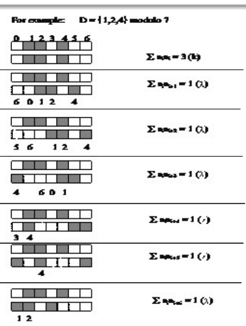

Spatial (Angular) Resolution

- Point or line spread function
- Modulation Transfer function (MTF)

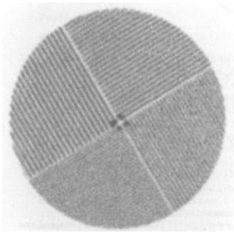

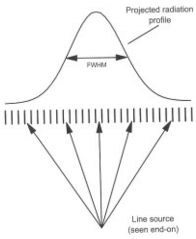

Progress in Performance

- Advances in Materials
- Advances in detectors
- Advances in methods

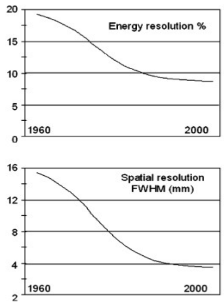

Modulation Collimators

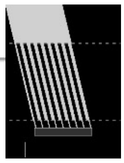

M. Oda first proposed linear scan modulation collimator (App. Opt. Vol.4 (1965) 143)

- Used to refine a location (e.g. galactic sky)
  - Like a vernier scale
- When the tilting angle θ changes by 2w/L, the triangular response function varies by one period. Choose w~0.1, L~ 40, arcmin

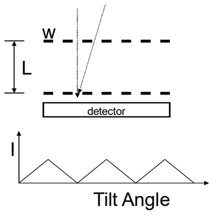

Rotational Modulation

- **Rotation modulation collimators**
  - L. Mertz (Proc. Symp. Modern Optics (1967)787-791.)
  - Angular resolution $\Delta\theta \approx \frac{w}{L}$
  - Signal-to-noise Ratio $SNR = \frac{1}{\sqrt{3}} \cdot \frac{S/4}{\sqrt{B}}$
    - where S = flux·Area·Time, B = b·A·t.
    - The factor 4 comes from the average transmission of 25%.
  - **The efficiency is significantly higher than a pinhole** (The effective area is 25% of detector area)
  - The source image (points) can be reconstructed using convolution (Zero-order Bessel functions) or Fourier transform techniques

Mechanical Multiplexing

G.K. Skinner / New Astronomy Reviews 48 (2004) 205–208 207

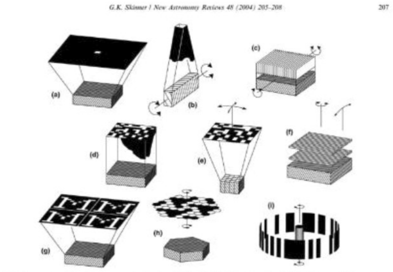

Fig. 2. Instruments with various degrees and types of multiplexing (coding). The extent of multiplexing increases in each row compared with the preceding one. Instruments in the left-hand column use only spatial coding and require a position sensitive detector. Those in the right-hand column use pure temporal coding and can operate with a single spatially unresolved detector element. Instruments in the central column utilise a mixture of the two. The types illustrated and one or more examples of each which have flown are: (a) pinhole camera (used in early solar experiments), (b) one-dimensional scanning pinhole camera (Ariel 5 ASM), (c) scanned collimated detector (Uhuru, Ariel 5 SSI, OSSE), (d) coded mask camera (TTM, Sigma), (e) coded mask with dithering (SPI; the RXTE ASM is also related to this class), (f) (rotation-) modulation collimator (RHESSI), (g) cyclic coded mask (SL2 XRT), (h) cyclic rotating coded mask (GRIP), (i) cyclic temporal coding (TGRS has flown with a very simple coding; GGAP has been proposed).

Coded Apertures

- Classic paper by Fennimore
- Derives cyclic difference sets
  - Cyclic autocorrelation function
    $$R_a(j) = \sum_{i=0}^{v-1} a_i \cdot a_{i+j}$$
- Shows 50% open is near optimal in many conditions
- Full pattern must appear to source, so mask pattern is repeated to ensure full shadow falls on detector
- Many mask choices
  - Uniformly redundant arrays (URAs)
  - Hexagonal URA (HURA)

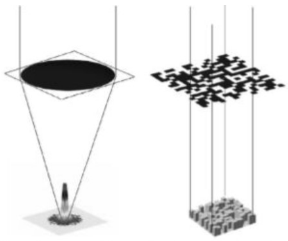

Fig. 1. Comparison of (a) an idealised imaging system with its point source response function (PSF) and (b) a coded mask telescope and its PSF.

Coded-Aperture Imaging

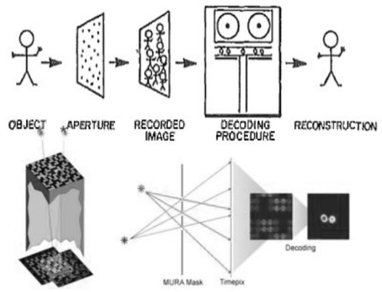

Radiation Imaging (Coded Aperture)

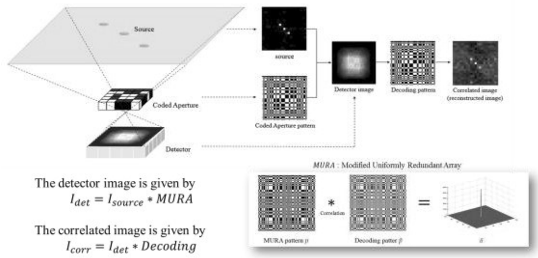

The detector image is given by
$I_{det} = I_{source} * MURA$

The correlated image is given by
$I_{corr} = I_{det} * Decoding$

Compton-scattering imagers (“Electronic collimation”)

- Compton scatter formula: $\cos\varphi = 1 - \frac{m_e c^2}{E_2} + \frac{m_e c^2}{E_1 + E_2}$

  Uncertainty in direction: $\Delta\varphi^2 = \Delta\varphi^2_{Energy} + \Delta\varphi^2_{Geometry}$

  and azimuthal uncertainty of 2π
- Better energy and position resolution improve the angular resolution.

  $\Delta E^2 = \Delta E^2_{Detector} + \Delta E^2_{Doppler}$

  - Doppler broadening: electron not at rest prior to the scattering
  - Explains why Compton edge not sharp
  - angular uncertainty due to Doppler
    - increases with Z, and
    - decreases with E_γ.
    - CZT: 140 keV: 5°; 511 keV: 1°

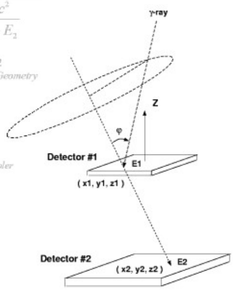

Gamma Imagers

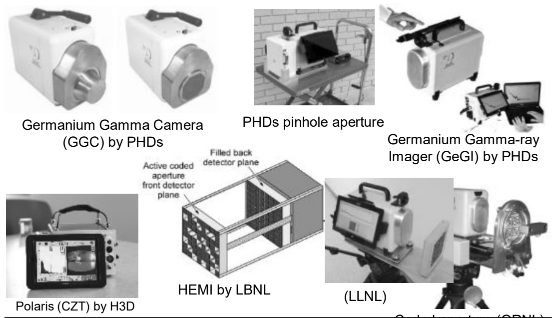

Germanium Gamma Camera (GGC) by PHDs

PHDs pinhole aperture

Germanium Gamma-ray Imager (GeGI) by PHDs

Polaris (CZT) by H3D

HEMI by LBNL

(LLNL)

Coded aperture (ORNL)

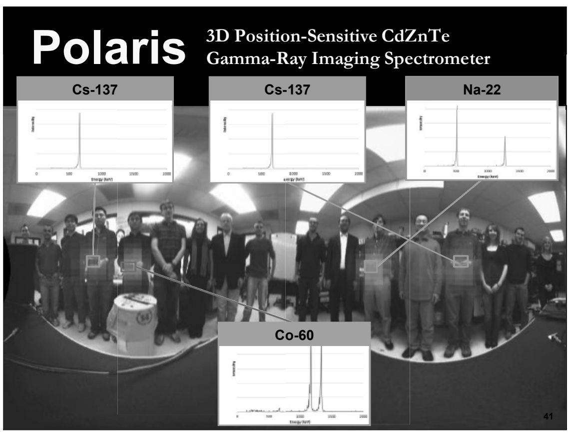

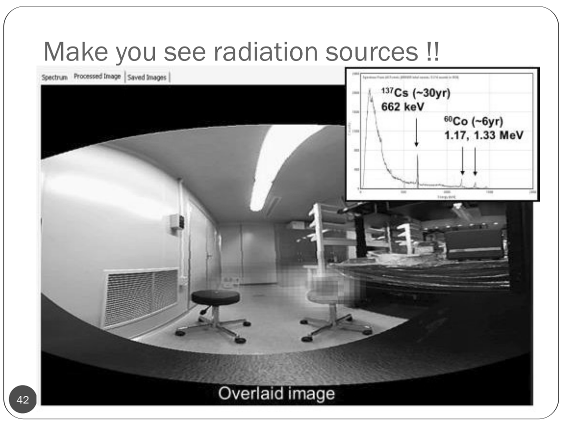

Tracking Moving Targets

An array of 3×3 (nine) 2×2×1.5 cm^3 CdZnTe tracks a moving ^{137}Cs

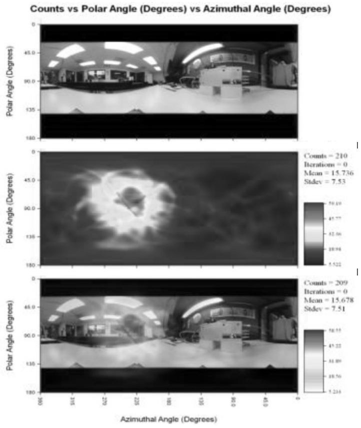

43

Finding Primary Radiation Sources

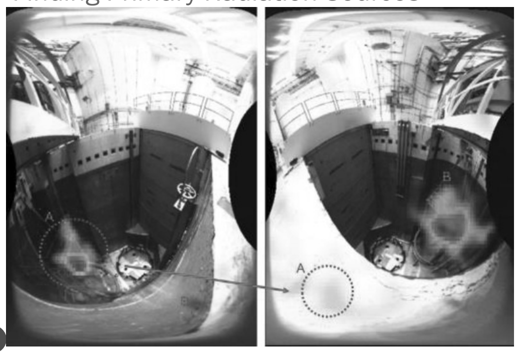

44

Decontamination & Clean-up Verification

- Measurement @ Fermi II NPP
- Provide information about the spatial content and distribution of radioactivity
- Hot area remains at drainage even after decontamination process

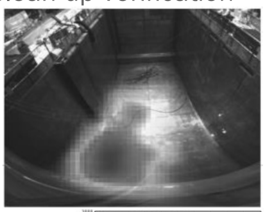

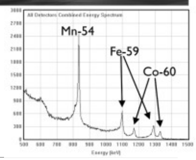

45

Locating Crud in Pipes and Valve

- Measurement @ Cook NPP
- Crud (metallic corrosion product) accumulated at bends of pipes and valve
- Hold-up Measurements

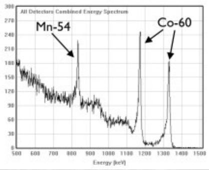

46

Locating Radioactivity in Shipping Containers

47

Electronic Collimation: Compton Camera (Compton Imaging)

Slides were provided by Prof. W. Lee from Korea University for Education Purpose.

SNU Nuclear Science

Compton imaging theory

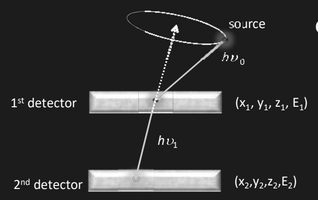

Compton Reconstruction

$$cos_\theta = 1 - \left(\frac{m_0c^2}{h\upsilon_0} \cdot \frac{E_1}{(h\upsilon_0 - E_1)}\right)$$

Courtesy of Prof. W. Lee from Korea University
Contents provided by educational purpose.

Compton imaging theory

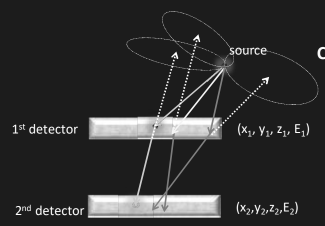

Compton Reconstruction

$$cos_\theta = 1 - \left(\frac{m_0c^2}{h\upsilon_0} \cdot \frac{E_1}{(h\upsilon_0 - E_1)}\right)$$

Courtesy of Prof. W. Lee from Korea University
Contents provided by educational purpose.

Compton imaging theory (structure)

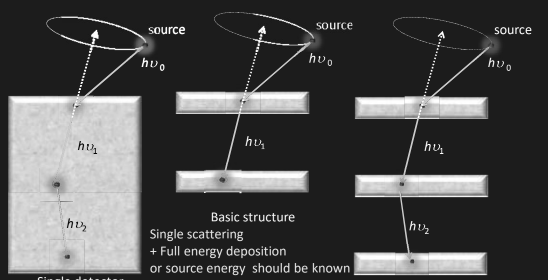

Single detector
Both single or
Multiple scattering is fine
Efficiency is very high.
Angular resolution can be low.

Basic structure
Single scattering
+ Full energy deposition
or source energy should be known

More than two detectors
No need full energy deposition
Efficiency is very low.

Compton imaging theory (detector)

Scintillator

Merit
. Can be made of large size (area) ∝ geometrical efficiency
. Fast timing -> low chance coincidence
. Room temperature operation
. Low cost (Conventional material)

Limit
. Low intrinsic efficiency
. Energy resolution is lower than that of semiconductor.

Compton imaging theory (detector)

Semiconductor

Merit
. Inner interactions can be analyzed – very high intrinsic efficiency
. Very high energy resolution – Precise energy identification
. Room temperature operation (CdZnTe or TlBr – YES, HPGe – NO)
. Portability (CdZnTe or TlBr – High, HPGe (cooling device) – Low)

Limit
. Timing resolution is lower than that of scintillator.
. High cost for a large single volume – Can be somewhat relieved

Compton imaging theory (detector)

Gas

Merit
. Track recoiled electron – Uncertainty of cone can be reduced.
. Large volume

Limit
. Very low efficiency
. Energy resolution is lower than that of semiconductor.

Compton imaging theory (Reconstruction)

Simple backprojection
. Fastest reconstruction but lowest angular resolution
. Real time imaging

Filtered backprojection
. The reconstruction method is **different** from that applied to CT
. Middle angular resolution but it takes time for reconstruction
. Real time imaging is possible if count rate is low

Iterative method (MLEM)
. Highest angular resolution but slow reconstruction
. It takes time for each iteration -> Real time ???
. Energy deconvolution is possible.

History of Compton Camera

Compton Camera started from astrophysical telescope to seek terrestrial sources and medical applications

"A telescope for soft gamma ray astronomy", Schonfelder (1973)
"A proposed γ camera", R. W. TODD (1974)
"Singe photon imaging with electronic collimation", Singh (1985)
"A ring Compton scatter camera for imaging medium energy gamma rays", Martin (1992)

Trend of Compton Camera

- **Detector Material**
  . Scintillator -> Semiconductor (+ gas???)
- **Converging with Other Technologies**
  . Visualization, GPS, Mobile (Drone)

Astrophysics

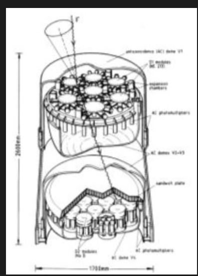

COMPTEL (NASA)

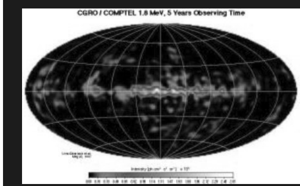

Liquid Scintillator (NE 213A) + NaI (Tl)
V. Schönfelder *et al.*, 1993, ApJ Suppl., **86**, 657 , http://heasarc.gsfc.nasa.gov/docs/cgro/comptel/

Astrophysics

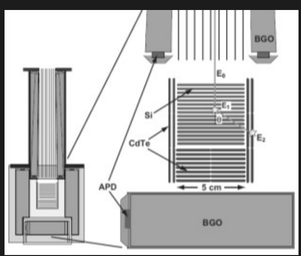

SGD (Univ. of Tokyo)

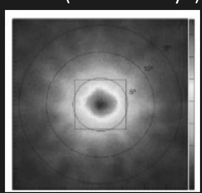

Yuto Ichinohe *et al.*, 2016, NIMA **806**, 5

Medical Application

C-SPRINT (Univ. of Michigan)

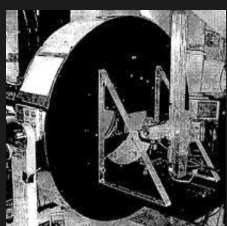

^{99m}Tc, point source, MLEM method

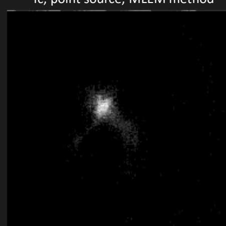

IEEE Trans. on Nuclear Science, 1999
IEEE Nuclear Science Symposium Conference Record, 1999.

Medical Application

Electron-Tracking Compton Camera
(Kyoto Univ.)

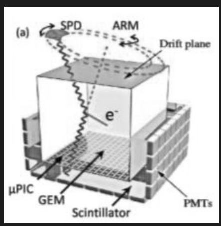

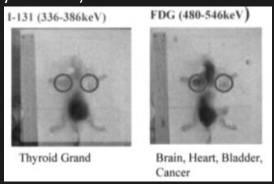

IEEE Nuclear Science Symposium Conference Record, 2008.

Medical Application

Compton camera for laparoscopic surgery (Univ. of Tokyo)

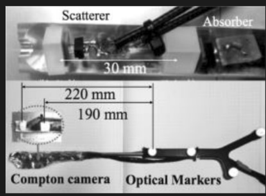

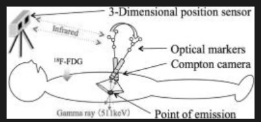

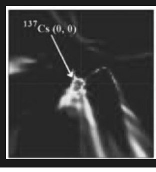

Detector: GAGG
A. Koyama *et al.*, 2017, NIMA **845**, 660

Medical Application

Compton camera for molecular imaging
(Waseda Univ., Hamamatsu)

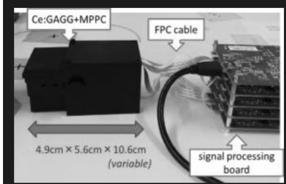

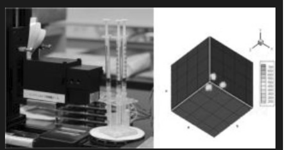

^{18}F, 3D image

A. Kishimoto *et al.*, 2017, NIMA **845**, 656

Medical Application

Handheld Compton Camera (Waseda Univ. + 3 institutes)

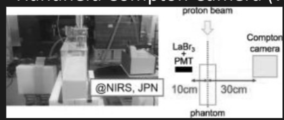

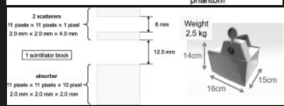

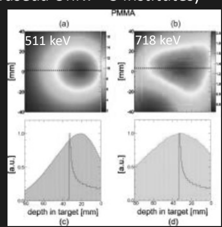

Online image, PMMA phantom

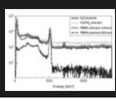

70 MeV , 3pA, 10 – 20min, proton beam
511 keV, positron, AR=8° for ^{137}Cs
718 keV, $^{10}B^*$
^{12}C, ^{16}O+p->$^{10}B^*$

Detector: GAGG
T. Taya *et al.*, 2016, NIMA **831**, 355

Medical Application

4.4 MeV r-ray imaging by 3D Compton Camera (Waseda Univ.)

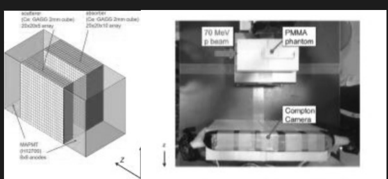

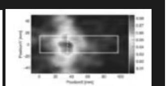

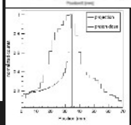

PMMA and $Ca(OH)_2$ and a 70 MeV, 0.3 pA, 4 hr proton beam, AR=10° for 4.4 MeV
Ayako Koide *et al.*, 2018, www.nature.com/scientificreports
Ayako Koide *et al.*, 2018, NIMA (in press)

KOREA UNIVERSITY

Cyber Knife

T. Lee and W. Lee, IEEE NSS-MIC-RSTD conference, San Diego, 2015
IEEE TNS, 63, No. 6, 2801-2806, 2016
PCT, USA No. 16/063,469

www.illinoisck.com

vetcyberknife.com

BNCT

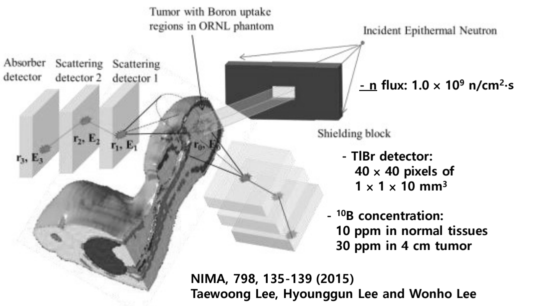

- n flux: 1.0×10^9 n/cm²·s
- TlBr detector: 40 × 40 pixels of 1 × 1 × 10 mm³
- ^{10}B concentration: 10 ppm in normal tissues, 30 ppm in 4 cm tumor

NIMA, 798, 135-139 (2015)
Taewoong Lee, Hyounggun Lee and Wonho Lee

Energy Spectrum and Images

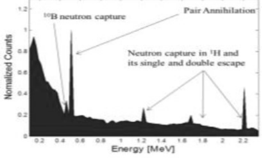

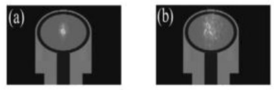

^{10}B: 478-keV, and (b) ^1H: 2200-keV.

. The yield of 478-keV γ-ray from ^{10}B is low but can be selectively reconstructed by energy window.
  -> High E resolution detector (Semiconductor) is required.

. To detect 478-keV and 2200-keV γ-ray, Compton imaging is effective.

. Image reconstruction: 5th iteration in MLEM method

Proton Therapy

- Proton intensity: 3.5×10^9
- Energy: 80, 150, 220 MeV
- Beam size: radius-0.25 cm

size: radius – 5, height – 40 cm

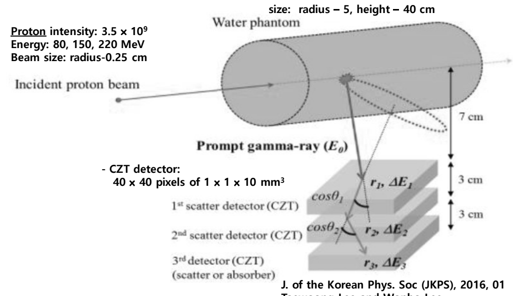

- CZT detector: 40 x 40 pixels of 1 x 1 x 10 mm³

J. of the Korean Phys. Soc (JKPS), 2016, 01
Taewoong Lee and Wonho Lee

Verification of Proton Range

Results	80 MeV	150 MeV	220 MeV
	Falloff position (mm)	Falloff position (mm)	Falloff position (mm)
Theoretical value (F2 tally)	52.2	159.0	309.4
Theoretical value (F6 tally)	52.0	158.5	308.5
SBP	54.5	163.5	312.5
FBP (n-value = 30)	53.0	162.5	311.5
MLEM (iteration = 18)	52.2	159.2	310.5

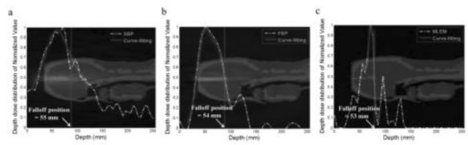

Compton PET

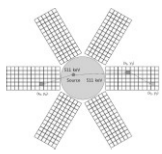

Schematic Diagram of Compton PET (CZT voxels)

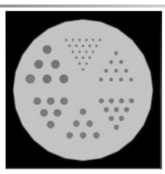

Micro-derenzo phantom

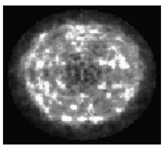

Conventional PET

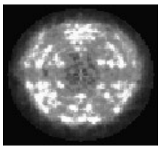

Compton PET

Changyeon *and* Wonho Lee *et al,*
(1) 2018, NT, 204, 386-395 (2) 2012, JKPS, 61,No.4, 626, (3) 2011, NIMA, 652, 713-716

Compton SPECT

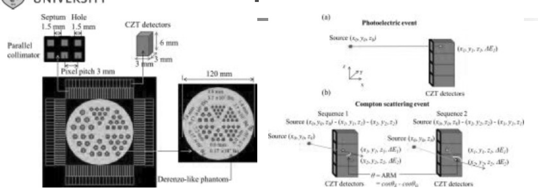

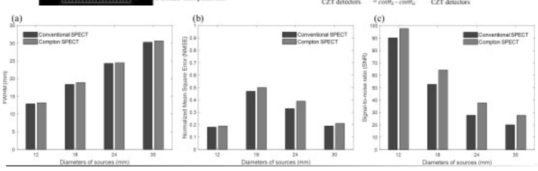

Taewoong Lee *et al.*, JKPS, 2018 , Vol. 73

Terrestrial Investigation

Pixelated LySO+MA-PMT, Monolithic NaI(Tl)+DSiPM
(Hanyang Univ. + KAERI)

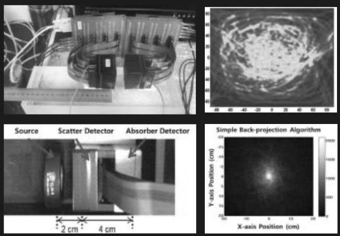

Pixelated LySO
+
MA-PMT

Monolithic NaI(Tl)
+
DSiPM

J. Park *et al.*, 2014, JKPS, **65**, No 9, 1360

Terrestrial Investigation

A portable 2xSi+3xCdTe Compton camera
(ISAS + 4 institute)

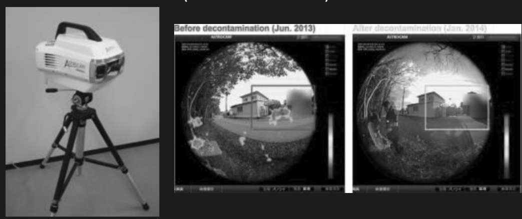

M. Kagaya *et al.*, 2015, NIMA, **787**, 207

Terrestrial Investigation

Low-cost-high sensitivity Compton Camera using CsI(Tl)
(Ibaraki Univ. + 5 institute)

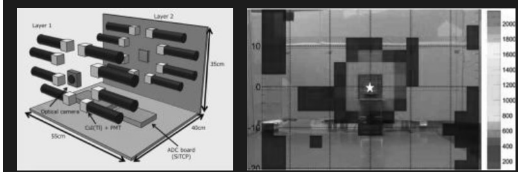

10 MBq
^{137}Cs

M. Kagaya *et al.*, 2015, NIMA, **804**, 25

Terrestrial Investigation

Compton camera mounted on an unmanned helicopter
(JAEA, Univ. of Tokyo, NICH, IMR)

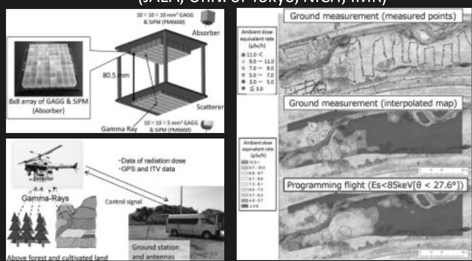

Fukushima

10 m
height

Yoshiaki Shikaze *et al.*, JNST, 2016, **53** (12), 1907

Terrestrial Investigation

Compton camera mounted on an mobile robot
(Univ. of Tokyo)

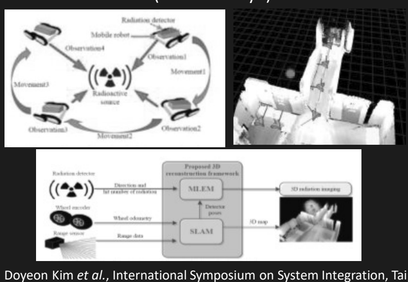

Doyeon Kim *et al.*, International Symposium on System Integration, Taipei, 2017

Terrestrial Investigation

- Polaris-H (H3D, Univ. of Michigan)

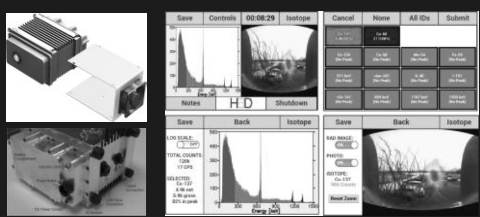

Christopher G. Wahl *et al.*, 2015, NIMA 784, 377

Terrestrial Investigation

Polaris-H with Robot

(Carnegie Mellon Univ.+Univ. of Michigan)

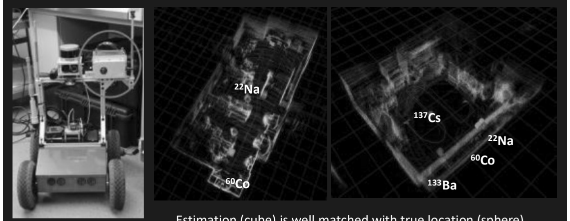

Estimation (cube) is well matched with true location (sphere)

Michael S. Lee *et al.*, 2018, WM2018 Conference, 2018

Terrestrial Investigation

HPGe Compton camera mounted on a cart

(UC Berkeley, LBNL)

Ross Barnowski *et al.*, 2015, NIMA, **800**, 65

Terrestrial Investigation

Handheld CdZnTe Compton camera

(UC Berkeley, LBNL)

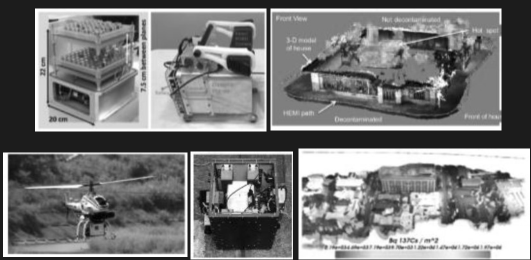

Kai Vetter, 2016, NIMA, 8**78**, 159

In addition……..

- Yi-Lin Liu et al, 'Preliminary results of a Compton camera based on a single 3D position-sensitive CZT detector', Nucl. Sci. and Tech. (2018)
- Optimization of the Compton camera for measuring prompt gamma rays in boron neutron capture therapy Chun-hui et al, ARI (2017)
  - Si (scatter) + Ge (absorber) detectors, Simulation

KOREA UNIVERSITY

4π FOV Compton Camera

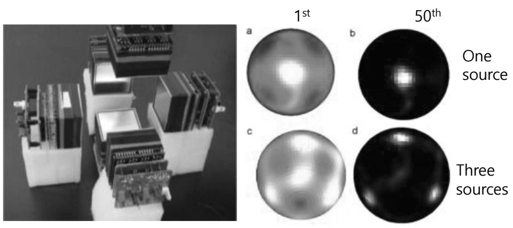

Intrinsic Efficiency : 4.67 x 10^{-4}

Radiation Measurement & Imaging Laboratory

Wonho Lee and Taewoong Lee, 2011, NIMA, 652, 33

KOREA UNIVERSITY

Hybrid Compton Camera

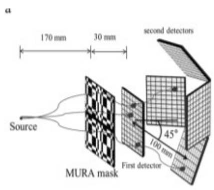

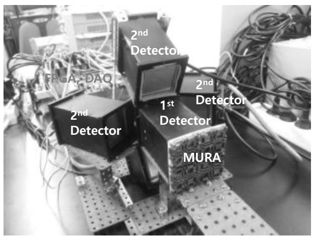

Radiation Measurement & Imaging Laboratory

Taewoong Lee and Wonho Lee., 2014, NIMA 767, No.11, 5

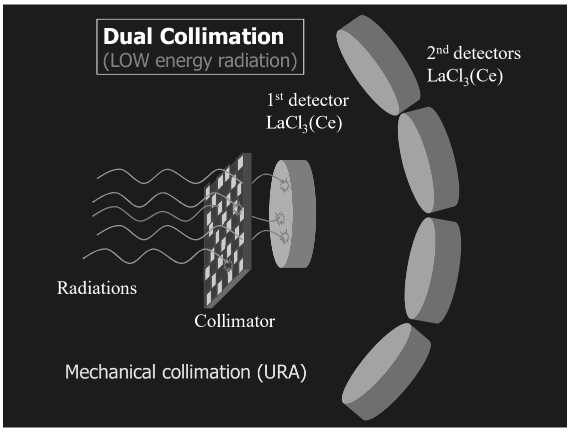

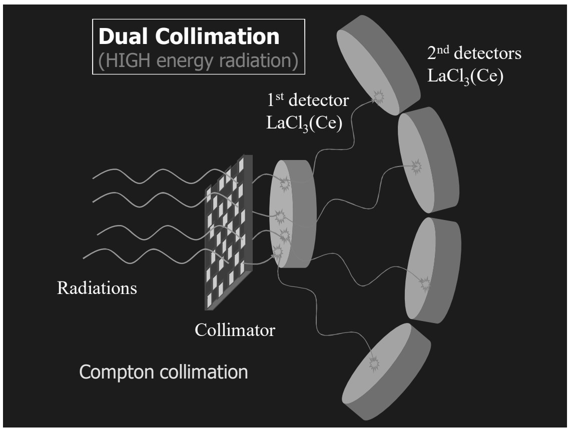

Image Combination: Maximum likelihood method

URA Compton

$$\lambda_j^{n+1} = \lambda_j^n \frac{\sum_i \frac{c_{ij}^U Y_i^U}{\sum_k c_{ik}^U \lambda_k^n} + \sum_i \frac{c_{ij}^C Y_i^C}{\sum_k c_{ik}^C \lambda_k^n}}{\sum_i c_{ij}^U + \sum_i c_{ij}^C}$$

c_{ij}: probability that a photon leaving j[th] cell reaches i[th] pixel
λ_j: source intensity of j[th] cell
Y_i: total number of events recorded for pixel i

Reconstructed Images

662 keV

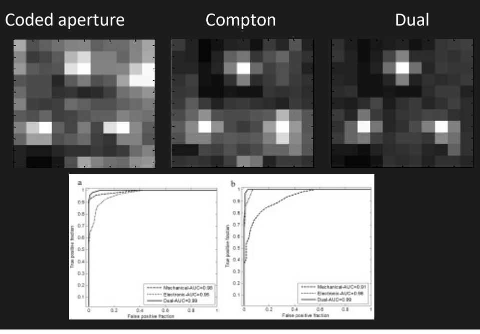

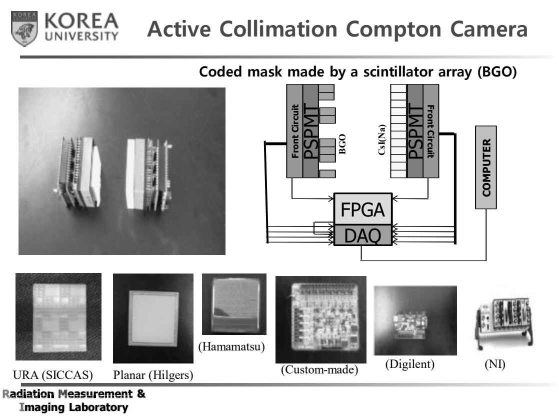

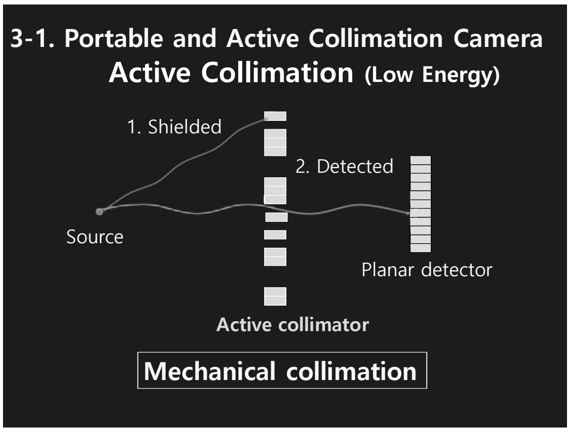

Active Collimation
(High Energy)

$\cos\theta_g = n_1 \cdot n_2$

$$\cos\theta_e = 1 - \frac{m_e c^2 E_r}{E_0 E_s} = 1 - \frac{m_e c^2 E_1}{E_0(E_0 - E_1)} \quad \text{if } E_0 \text{ is known}$$

$$= 1 - \frac{m_e c^2 E_1}{(E_1 + E_2)E_2} \quad \text{if } E_0 \text{ is unknown and } E_0 = E_1 + E_2$$

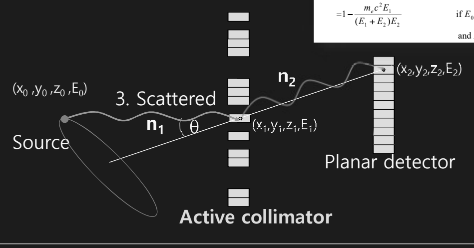

Electronic collimation:
Scattered radiations in the active collimator are also effective events

Schematic Diagram and Equipment

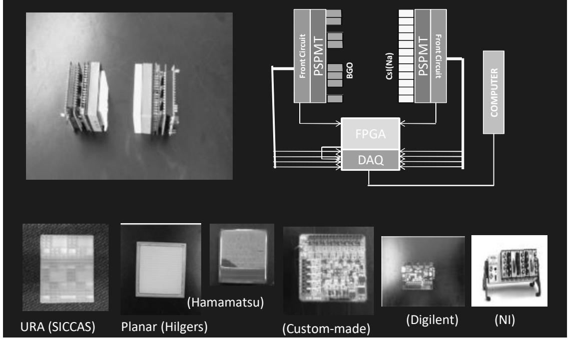

Mechanical Collimation: Coded-Aperture

Slides were provided by Prof. M. Jeong from Jeju University for Education Purpose.

Coded-Aperture Imaging

- **Coded Aperture Imaging**
  - Technique originally developed for X-ray astronomy
  - Can achieve the resolution of small pinholes while maintaining a high signal throughput
  - Technique that seeks to overcome the normally poor SNR in X-ray imaging using pinhole or collimators
- **Current Applications**
  - **Radioactive material localization**: Homeland Security, Nuclear Safety, Nuclear Safeguards, Environmental Monitoring
  - **Near-field coded aperture imaging at nuclear fields**: Gamma & Neutron imaging for accelerator and cyclotron's monitoring and safety

Coded-Aperture vs. Compton

	Coded Aperture (SiPM or CdTe)	Compton Camera (CZT)
Field of View	45°-50°	Up to 360°
Angular Resolution	2.5° - 6°	10° - 30°
Energy Range	30 keV – 10 MeV (1.5 MeV)	250 keV – 1.5 MeV
Dose Linearity	2 μSv/h – 10 Sv/h	N/A
Sensitivity	2 nSv/h ^{241}Am in 2 min.	30 nSv/h ^{137}Cs in 5 min.
Energy Resolution	Very limited by detector	High (~1%)

- IAEA Symposium on International Safeguards, 20-24 Oct. 2014 (Vienna), Presented by CANBERRA

#4

Example of Compton Camera

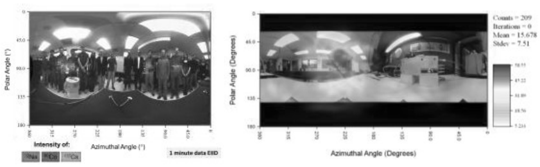

From Z. He's Presentation at IEEE RTSD 2010

Coded-Aperture Imaging

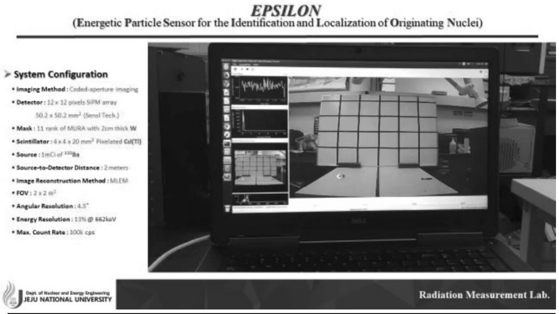

Hardware Configuration

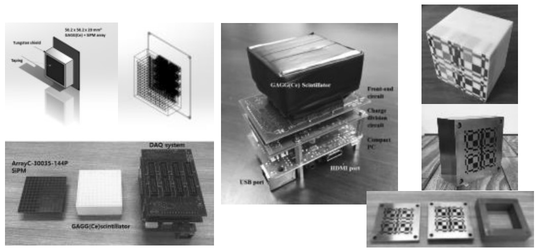

System Outline

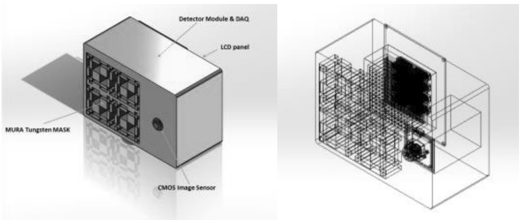

Radiation Imaging (Coded Aperture)

Mechanical Collimation: (Temporal Modulation)

Rotational Modulation

Radiation Imaging Technique

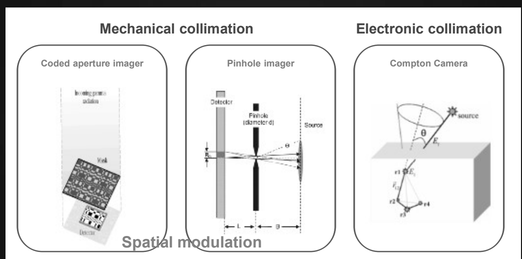

K. Vetter *et al*., "Gamma-ray Imaging Methods," Lawrence Livermore National Laboratory, UCRL-TR-225239, 2006.

Requires <u>position-sensitive detectors</u>

What is the RMC?

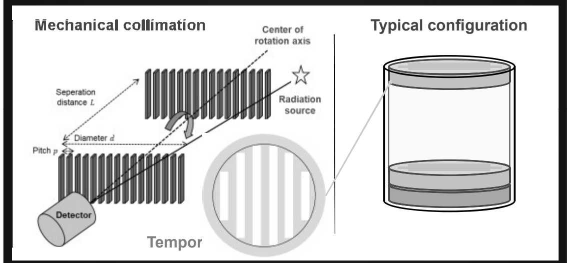

Non-position-sensitive detector

Indirect Imaging: Modulation Patterns

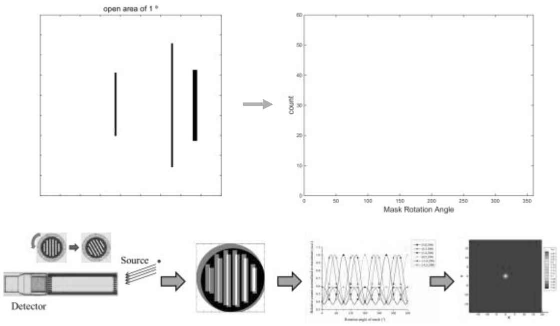

Previous RMC Studies

Univ. Michigan

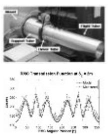

Gamma-ray source	Target materials	Neutron /gamma-ray Sources
NaI scintillator	Detector	CLYC scintillator
9°	FOV	18°

Sejong Univ.

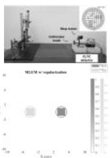

- University of Michigan
  - Orphan source search problem (only gamma-ray source detection)
  - Development of universal field model to predict the RMC response (*Nucl. Instr. And Meth. A 2009, 2011*)
- Sejong Univ.
  - Neutron/gamma-ray dual particle imaging system
  - Design of a new bilateral asymmetric mask design (*JRR 2018, CAP 2019*)

4

Field-of-View Extension

- In order to overcome the limited FOV
  - A new **hemispherical collimator** design which can extend the **FOV to approximately 2π**
  - Demonstrating the imaging capability of hemispherical RMC system via measurement experiments

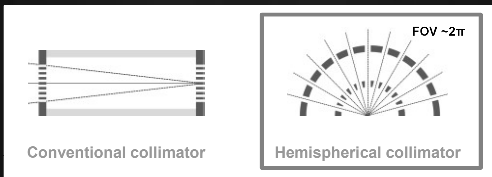

106

Methods: H-RMC System Configuration

H-RMC System

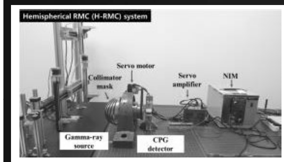

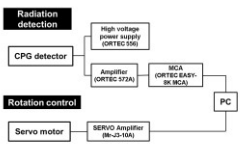

1) Collimator mask design

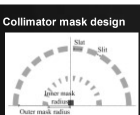

-slat/slit interval: 7˚
-outer mask radius: 9.5 cm
-inner mask radius: 2.5 cm
-0.5 cm-thick stainless-steel mask

2) CZT-based CPG detector

Detector size	10×10×10 mm^3
Resolution	4.4% @356 keV
	3.6% @662 keV
Intrinsic peak efficiency	66.8% @356 keV
	22.8% @662 keV
Energy range	30 to 1.3 MeV
Operating tem.	+10 to +35℃

Coplanar grid-type CZT detector (Kromek Group plc, UK)

3) Rotation Control System

Proportional–Integral–Derivative controller controller

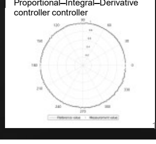

107

Results: Complex Gamma-ray Environment

- ^{133}Ba source1 position (r,θ,φ): (25 cm, 40°, 30°)
- ^{133}Ba source2 position (r,θ,φ): (15 cm, 20°,180°)
- ^{137}Cs source position (r,θ,φ): (20 cm, 30°,180°)
- Dwell time: 40 min
- Rotation interval: 10˚

Radionuclide	Source type	Activity (kBq)	Reference date
^{133}Ba(1)	D-type	3312.2	01-Aug-2018
^{133}Ba(2)	R-type	393.7	01-Apr-2016
^{137}Cs	R-type	378.5	01-Apr-2016

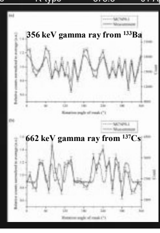

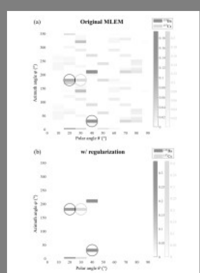

Complex sources environment	SNR		SSIM	
	Ori	Regul	Ori	Regul
356 keV image	12.69	18.47	0.89	0.92
662 keV image	17.06	23.64	0.93	0.96

12

Dual-Particle Imaging (Recent Approaches)

Neutron Imaging

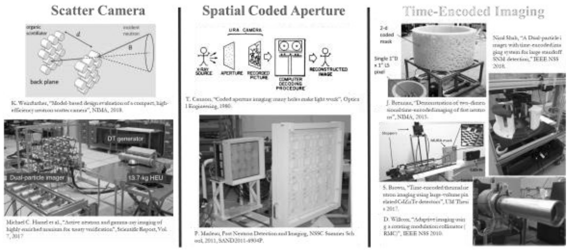

Neutron Imagers

MINER fast neutron scatter camera by SNL

High sensitivity directional radiation detection system (rotating) by SNL

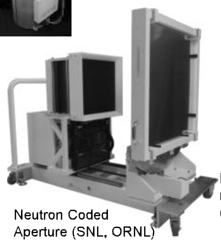

BNL Thermal Neutron

Neutron Coded Aperture (SNL, ORNL)

Special Nuclear Material Detection Methods

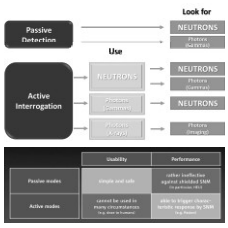

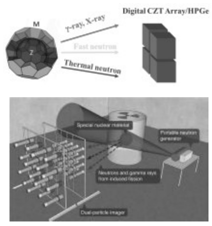

Dual-particle Imaging (DPI) System

- Neutrons and gamma rays are two signatures of **special nuclear materials (SNM)**
  - Photons can be significantly attenuated with high-Z material
  - Neutrons can easily penetrate high-Z materials, but Low-Z materials are effective at moderating neutrons

Gamma–neutron imaging system
(RMD, USA)

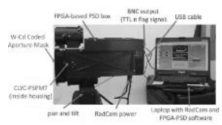

- **Concept of coded aperture imaging**
- CLYC scintillator with PSPMT

Dual-Particle Imaging (DPI) System
(Univ. Michigan, USA)

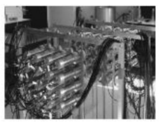

- **Concept of Compton imaging**
- 3 planar arrays of 16 detectors (Liquid and NaI(Tl) scintillators)

C.M. Whiney *et al.*, "Gamma–neutron imaging system utilizing pulse shape discrimination with CLYC," *Nucl. Inst. and Met. A*, 2015.
A.P. Poitrasson-Riviere *et al.* "Dual-particle imaging system based on simultaneous detection of photon and neutron collision events," *Nucl. Inst. and Met. A*, 2014.

Motivations for DPI

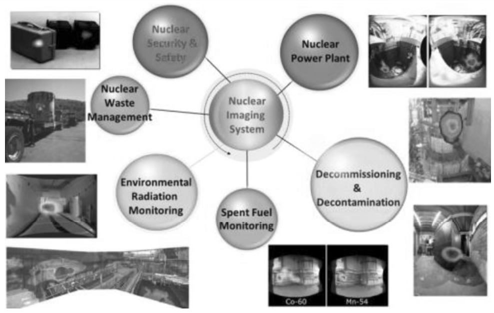

Stilbene Crystal

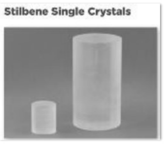

Chemical Formula:	$C_{14}H_{12}$
Crystal Symmetry:	monoclinic
Optical Symmetry:	biaxial
Class:	$P2_1/c$

Features	Advantages
Direct detection of fast neutrons	• Neutrons do not need to be moderated to lower energies. • Measurements can take advantage of the low background, long attenuation length, and minimal number of benign sources of fast neutrons.
Excellent discrimination between neutrons and gamma rays	• Facilitates counting fast neutrons without false positives from gamma rays. • Permits use of lower energy thresholds.
Solid, non-hygroscopic, not flammable, not hazardous	• Unpackaged stilbene is stable. • Avoids the transportation, storage, and handling concerns of many liquid organic scintillators.

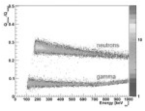

Scintillation Peak	390 nm
Melting Point	124 °C
Refractive Indices (at 589 nm)	1.703, 1.724, 1.844
Density	1.15 g/cm³

Example of Stilben + SiPM signals

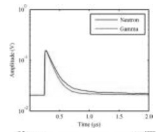

Table 1. Optimized PSD parameters.

Configuration	Total start time (ns)	Tail start time (ns)	Integral end time (ns)
PMT	2	18	300
B-Series SiPM	2	34	520
C-Series SiPM	0	44	1100

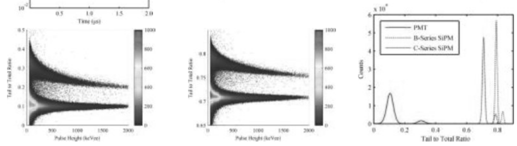

Coded Aperture based DPI

Dual Particle Imager (DPI) –MCNP simulated

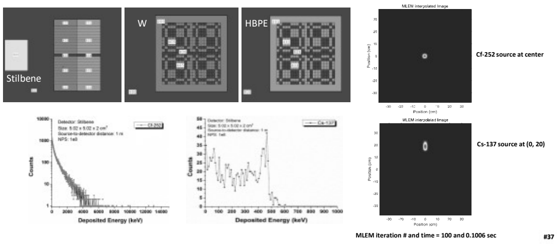

RMC-based Dual-Particle Imager

- Rotational Modulation Collimator (RMC)
  - Originally developed for X-ray and solar flare imaging in astronomy.
  - Does not require a position-sensitive radiation detector.
  - As collimators rotate, the open area made by slits change over time.

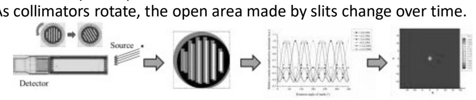

- PSD-capable Scintillators

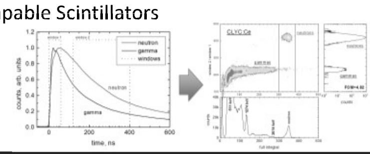

RMC-based Dual-Particle Imager

Gamma-ray Measurement and Imaging with RMC

- Radiation Imaging with RMC
  - Asymmetric Mask (Pb 1 cm+ BPE 0.2 cm)
  - Distance from RMC to source: 1 m
  - Sources: ^{137}Cs 10.23 μCi, ^{133}Ba 10.64 μCi (reference date 2016-04-01)

<Rotational modulation patterns for Cs-137>

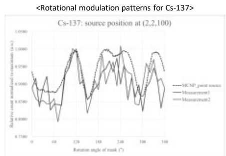

<Reconstructed images for gamma-ray source>

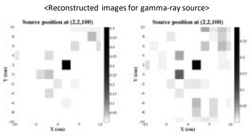

MLEM iteration 5,000

Results: Reconstructed Image

- ^{133}Ba Source position: (-5 cm, 0 cm,100 cm)
- ^{137}Cs Source position: (5 cm, 0 cm,100 cm)

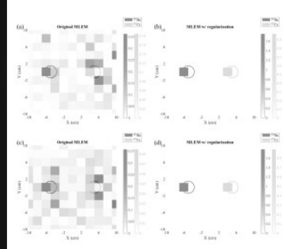

	SNR		SSIM	
	Original MLEM	MLEM with regularization	Original MLEM	MLEM with regularization
356 keV image (Measurement1)	17.04	28.25	0.69	0.98
356 keV image (Measurement2)	16.9	28.00	0.69	0.98
662 keV image (Measurement1)	9.38	49.06	0.63	1.00
662 keV image (Measurement2)	5.98	39.08	0.58	1.00

Signal-to-noise ratio (SNR)
Structural similarity (SSIM) index

Results: Reconstructed Image

- ^{137}Cs Source position: (-4 cm, 0 cm,100 cm)
- ^{252}Cf Source position: (4 cm, 0 cm,100 cm)

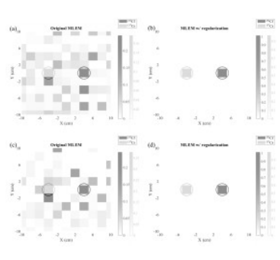

	SNR		SSIM	
	Original MLEM	MLEM with regularization	Original MLEM	MLEM with regularization
662 keV image (Measurement1)	9.12	49.70	0.63	1.00
662 keV image (Measurement2)	16.21	60.70	0.75	1.00
Neutron image (Measurement1)	12.54	59.31	0.68	1.00
Neutron image (Measurement2)	13.14	61.31	0.67	1.00

Signal-to-noise ratio (SNR)
Structural similarity (SSIM) index

Related on-going works: Imaging Methods

- **Non-Local Means (NLM) filter: Image enhancement technique**

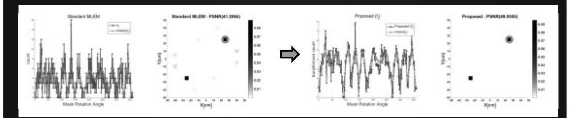

- **Deep-learning in Image Reconstruction: CNN vs. GAN**

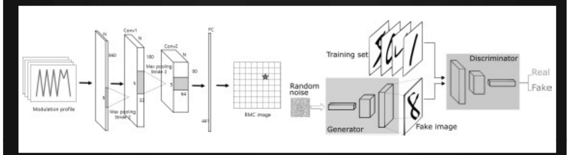

Courtesy of Sohyun Park and Gyemin Lee (SeoulTech)

Active Interrogation Imagers

FNMIS – Fieldable Nuclear Materials Inspection System by ORNL

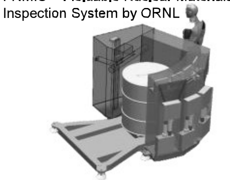

Associated Particle Imaging (API) neutron generators

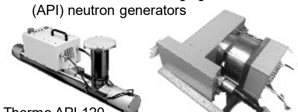

Thermo API 120
Optical alpha detector
$5x10^7$n/s

Russian ING-27
Solid state alpha detector
$1x10^8$n/s

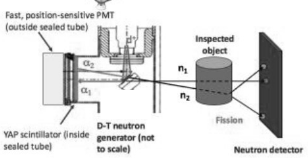

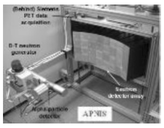

APNIS – Advanced Portable Neutron Imaging System (ORNL)

Imaging Technology

- **Gamma - CZT, HPGe, NaI?**
  - Isotope ID, Gamma source localization and geometry
- **Thermal neutron – ^{3}He and replacements**
  - Location and low resolution image of thermal neutron source (shielded sources)
- **Fast neutron – liquid, plastic, crystal scintillators**
  - Pulse shape discrimination (PSD) – neutron, gamma, etc.
  - Particle identification, low resolution neutron spectroscopy, location of and geometry of fast neutron source
- **Combinations + Contextual Sensing**
- **Muon**
- **Active Neutron Interrogation**
  - Transmission
  - Elastic scatter
  - Tomography – multiple points of view
- **X-Ray**

Imaging Modes
- **Pinhole**
- **Coded Aperture**
- **Compton Scatter (> 500 keV)**

Things to Consider

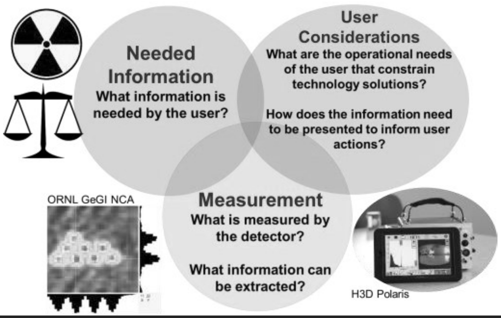

User Considerations

- Power needs
  - Wall plugin, vehicle plugin, battery
- Size / Footprint
  - Fixed, transportable, pallet, vehicle, backpack / man portable
- Transportability
- Time
  - Detect and identify (location, material, shape)
- Data management
  - Automated analysis
  - Information provided to the user
  - Data transfer

- **User Interface**
  - Information provided to the user
  - Frequency of data display
    - Real time
    - Completion of measurement
- **Concept of Operations**
- **Complexity**
  - Passive versus active
  - Ease of use
  - Robustness

Considerations in Measurement

- Detection efficiency
  - Time to detect
  - Time to measure characteristic (location, size, material, shape, etc.)
- Background rejection
- Energy resolution
- Energy range
- Particle identification
- Field of view
- Angular resolution
- Spatial resolution (3D)
  - Depth
- Contrast

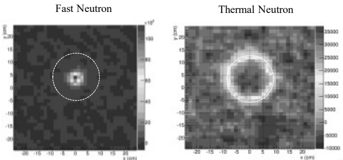

ORNL/SNL Neutron Coded Aperture

Applications of Radiation Imaging

1. Applied to Photon Therapy

Cyber Knife

T. Lee and W. Lee, IEEE NSS-MIC-RSTD conference, San Diego, 2015
IEEE TNS, **63**, No. 6, 2801-2806, 2016
PCT, USA No. 16/063,469

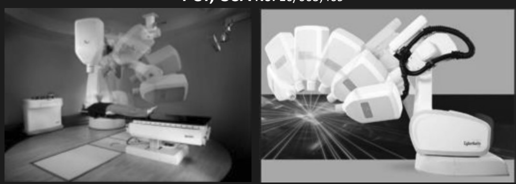

www.illinoisck.com vetcyberknife.com

Conventional EPID

Incident 6-MV Photon

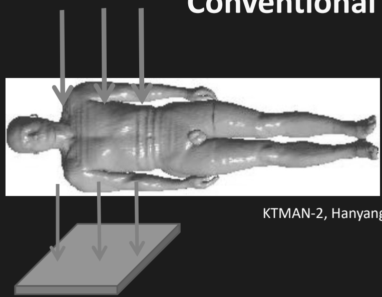

KTMAN-2, Hanyang Univ.

Limited angle for imaging (projected direction only)
Difficult to apply mechanical collimation (High energy)

New method Compton imaging

Incident 6-MV Photon

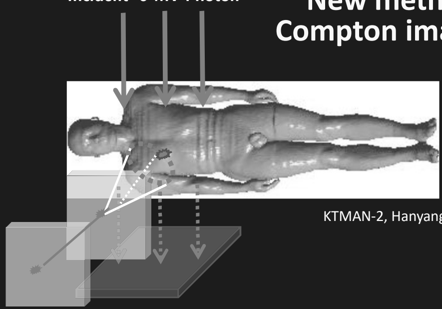

KTMAN-2, Hanyang Univ.

Full angle measurement based on the reconstruction of scattered radiations
Compton camera is preferable for high energy (~MeV)

New method + Back calculated dose

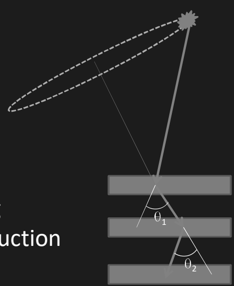

General
Multiple Scattering
Compton Reconstruction

It finds where the source come from.
based on detected position and energy information

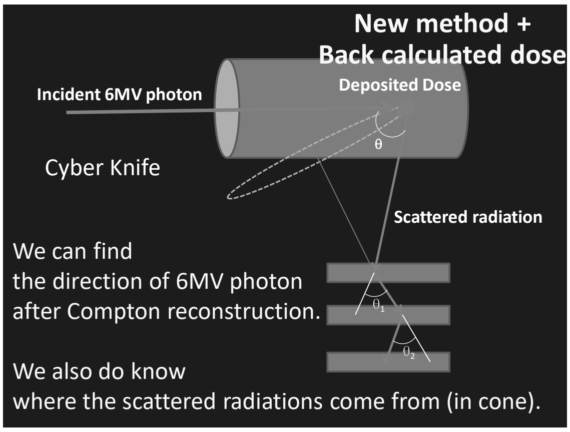
New method +
Back calculated dose
Incident 6MV photon
Deposited Dose
θ
Cyber Knife
Scattered radiation
We can find
the direction of 6MV photon
after Compton reconstruction.
We also do know
where the scattered radiations come from (in cone).
θ_1
θ_2

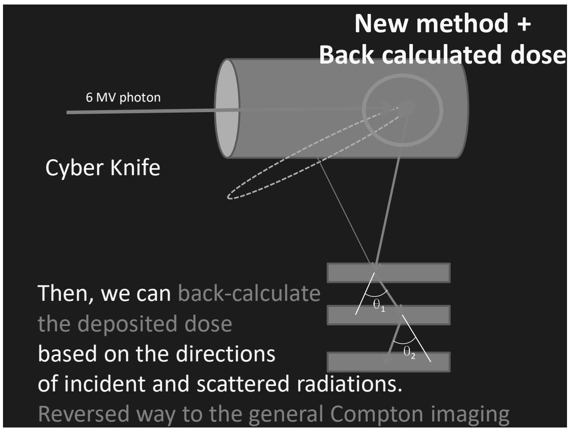
New method +
Back calculated dose
6 MV photon
Cyber Knife
Then, we can back-calculate
the deposited dose
based on the directions
of incident and scattered radiations.
Reversed way to the general Compton imaging
θ_1
θ_2

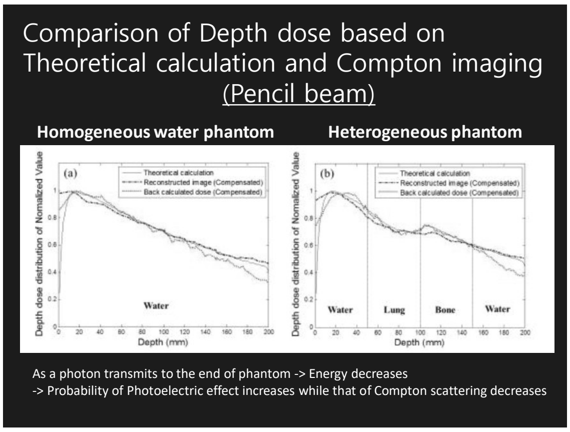
Comparison of Depth dose based on
Theoretical calculation and Compton imaging
(Pencil beam)
Homogeneous water phantom
Heterogeneous phantom
(a)
(b)
Theoretical calculation
Reconstructed image (Compensated)
Back calculated dose (Compensated)
Depth dose distribution of Normalized Value
Depth (mm)
Water
Water Lung Bone Water
As a photon transmits to the end of phantom -> Energy decreases
-> Probability of Photoelectric effect increases while that of Compton scattering decreases

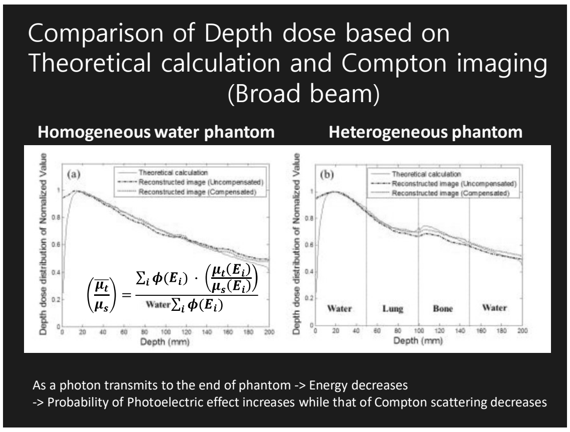
Comparison of Depth dose based on
Theoretical calculation and Compton imaging
(Broad beam)
Homogeneous water phantom
Heterogeneous phantom
(a)
(b)
Theoretical calculation
Reconstructed image (Uncompensated)
Reconstructed image (Compensated)
Depth dose distribution of Normalized Value
Depth (mm)
$\left(\frac{\mu_t}{\mu_s}\right)_{Water} = \frac{\sum_i \phi(E_i)\cdot\left(\frac{\mu_t(E_i)}{\mu_s(E_i)}\right)}{\sum_i \phi(E_i)}$
Water Lung Bone Water
As a photon transmits to the end of phantom -> Energy decreases
-> Probability of Photoelectric effect increases while that of Compton scattering decreases

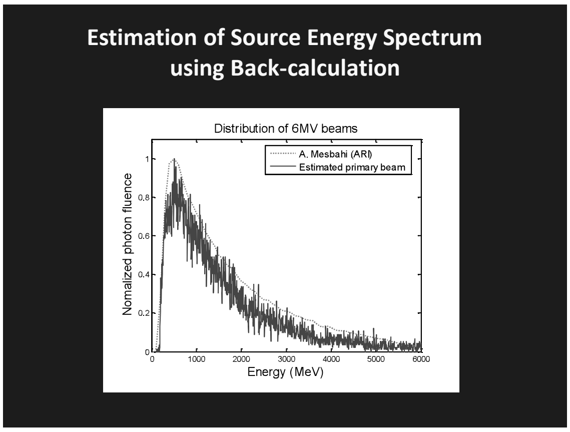
Estimation of Source Energy Spectrum
using Back-calculation
Distribution of 6MV beams
A. Mesbahi (ARI)
Estimated primary beam
Nomalized photon fluence
Energy (MeV)

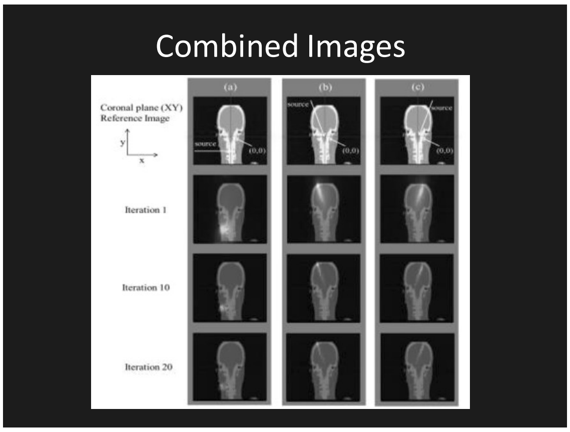
Combined Images
(a)
(b)
(c)
Coronal plane (XY)
Reference Image
source
(0,0)
Iteration 1
Iteration 10
Iteration 20

2. Applied to BNCT

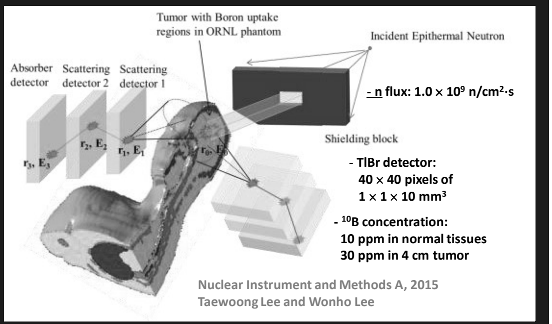

Simulated Spectrum and image

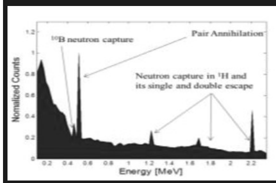

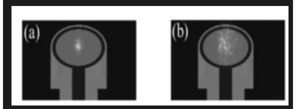

^{10}B: 478-keV, and (b) ^{1}H: 2200-keV.

. The yield of 478-keV γ-ray from ^{10}B is low but can be selectively reconstructed by energy window.
-> High E resolution detector (Semiconductor) is required.

. To detect 478-keV and 2200-keV γ-ray, Compton imaging is effective.

. Image reconstruction: 5th iteration in MLEM method

Angular Resolution

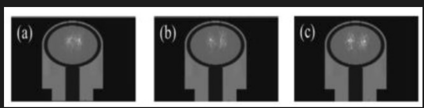

(a) 1 cm (b) 2 cm (c) 3 cm

Image reconstruction: 5th iteration in MLEM method

When the distance between BURs was greater than 2 cm, the BURs were distinguishable.

3. Applied to Proton therapy

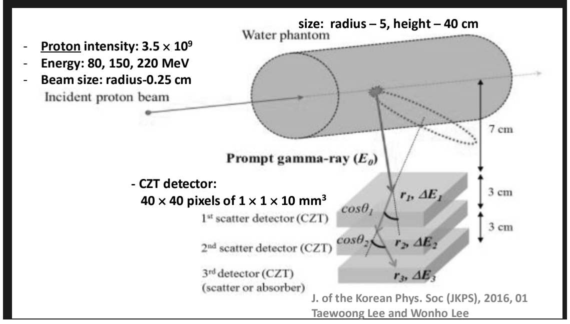

Comparison of the falloff positions of the Bragg peak (Water phantom)

Multiple-scattering Compton Imagers (MSCIs) vs.
Theoretical value (F2 or F6 tally): flux of prompt γ-ray in the water phantom
(ref. C. H. Min *et al*. Med. Phys, 2012)

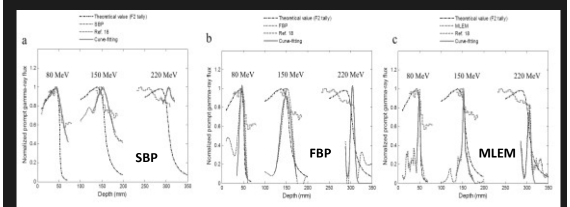

N-value: 30 (FBP), iteration: 18 (MLEM)

Comparison of the falloff positions of the Bragg peak (Water phantom)

Results	80 MeV	150 MeV	220 MeV
	Falloff position (mm)	Falloff position (mm)	Falloff position (mm)
Theoretical value (F2 tally)	52.2	159.0	309.4
Theoretical value (F6 tally)	52.0	158.5	308.5
SBP	54.5	163.5	312.5
FBP (n-value = 30)	53.0	162.5	311.5
MLEM (iteration = 18)	52.2	159.2	310.5

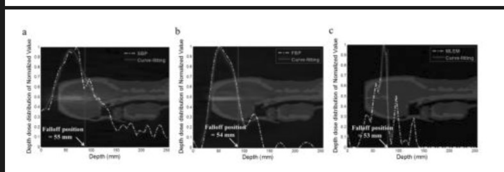

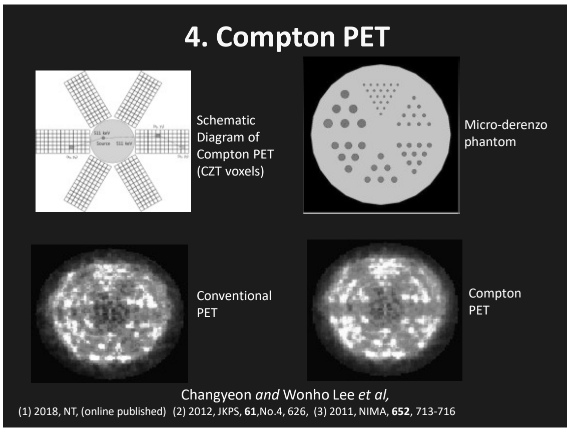
4. Compton PET
Schematic Diagram of Compton PET (CZT voxels)
Micro-derenzo phantom
Conventional PET
Compton PET
Changyeon and Wonho Lee et al,
(1) 2018, NT, (online published) (2) 2012, JKPS, 61,No.4, 626, (3) 2011, NIMA, 652, 713-716

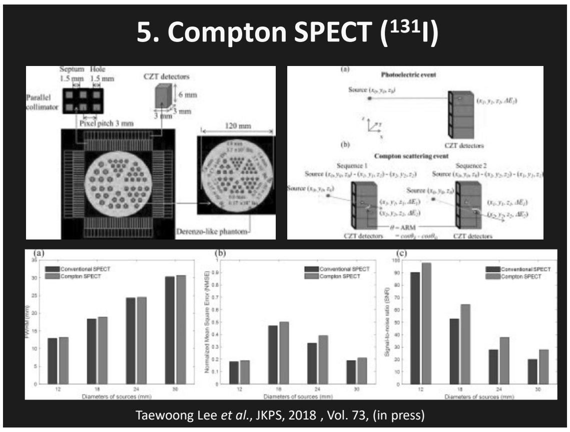
5. Compton SPECT (131I)
Septum 1.5 mm
Hole 1.5 mm
CZT detectors
Parallel collimator
6 mm
3 mm
Pixel pitch 3 mm
120 mm
Derenzo-like phantom
Photoelectric event
Compton scattering event
Sequence 1
Sequence 2
CZT detectors
Conventional SPECT
Compton SPECT
Diameters of sources (mm)
Taewoong Lee et al., JKPS, 2018 , Vol. 73, (in press)